

## Mesoscopic theory of the viscoelasticity of polymers

Shirish M. Chitanvis

*Theoretical Division, Los Alamos National Laboratory, Los Alamos, New Mexico 87545*

(Received 13 October 1998; revised manuscript received 8 June 1999)

We have advanced our previous static theory of polymer entanglement involving an extended Cahn-Hilliard functional, to include time-dependent dynamics. We go beyond the Gaussian approximation, to the one-loop level, to compute the frequency dependent storage and loss moduli of the system. The four parameters in our theory are obtained by fitting to available experimental data on polystyrene melts of various chain lengths. This provides a physical representation of the parameters in terms of the chain length of the system. It is shown that the parameters chosen describe the crossover from an unentangled to an entangled state. The crossover is characterized by a dramatic increase in a time scale appearing in the theory, analogous to critical slowing down in phase transition theory. This result should stimulate more detailed experiments in this regime to test this concept. [S1063-651X(99)07809-5]

PACS number(s): 61.41.+e, 83.10.Nn

In a previous paper, we developed a static field theory of polymer entanglement [1], in which we introduced a nonlocal attractive term, in addition to the usual excluded volume term, that models resistance to the motion of polymers due to entanglement. Starting with this energy functional, we were able to use renormalization group techniques to describe the onset of entanglement as the average molecular weight is increased to a critical value. The onset of entanglement was described as a cross-over phenomenon, characterized by a parameter which plays the role of a diffusion constant, going to zero as the transition point is approached. This was interpreted as an indication of critical slowing down.

There have been several numerical approaches developed to understand the viscoelastic response of polymers [2–4]. It is of interest to see whether an alternative theory of viscoelasticity of polymers using continuum concepts can be developed. Our previous theory, being static in nature, clearly needs to be extended if one is to study the time-dependent response of polymeric systems. The chief purpose of this paper is to lay down the foundations of a time-dependent field theory of entangled polymers through a comparison with experimental results on the linear viscoelastic response of polymer melts. In so doing we have probed the time-dependent approach to entanglement of polymeric systems, as the molecular weight is increased to a critical value. The onset of entanglement is analogous to dynamic critical phenomena, where the characteristic frequency scales to zero as the transition is approached. This is an aspect of the onset of entanglement which deserves further investigation.

The time-dependent internal energy functional  $U$  which extends our previous static theory [1] can be written down in a straightforward manner in terms of an energy density  $u$ :

$$U = \int d^3s \int_{-\omega_m}^{\omega_m} \frac{d\omega}{2\pi} u(\mathbf{s}, \omega), \quad (1)$$

$$\begin{aligned} \beta u = & c(\mathbf{s}, -\omega)(-i\omega)c(\mathbf{s}, \omega) + \left(\frac{\alpha}{\sqrt{2}}\right) \vec{\nabla}_s c(\mathbf{s}, -\omega) \cdot \vec{\nabla}_s c(\mathbf{s}, \omega) \\ & + \left(\frac{\alpha^2}{2}\right) c(\mathbf{s}, -\omega)c(\mathbf{s}, \omega) \\ & - \left(\frac{\alpha^4}{2\pi}\right) \int d^3s' c(\mathbf{s}, -\omega) \frac{\exp(-\delta|\mathbf{s}-\mathbf{s}'|)}{|\mathbf{s}-\mathbf{s}'|} c(\mathbf{s}', \omega) \end{aligned}$$

$$\beta = \frac{1}{kT},$$

where  $c$  is the number concentration of the polymer strands and  $\delta^2 = \sqrt{2}\alpha$ ,  $k$ , is Boltzmann's constant, and  $T$  is the absolute temperature. The model is an extension of the standard Cahn-Hilliard approach [6].  $\alpha$  plays a role analogous to that of a diffusion constant. The third term in the equation represents the standard excluded volume interaction. The final nonlocal attractive term represents the fact that when polymers become entangled, there will be in general a resistance to their movement. Similar approaches can be found in the literature, where authors have taken activation energies to represent entanglement [3]. The form of our interaction term is novel, however, and we have discussed in the previous paper [1] the rationale for the manner in which the parameter  $\alpha$  appears in the model is as given in that paper, since it leads to a number-preserving Euler-Lagrange equation. It is worth noting that standard treatments involve just the excluded volume term and are restricted to the static case, whereas we have considered here an extension to the time-dependent case as well. The limits on the frequency integral  $\pm\omega_m$  indicate an inverse (maximum) time scale which characterizes the system. The first two terms on the right-hand side of Eq. (1) by themselves yield the diffusion equation in the mean-field approximation in the limit that  $\omega_m \rightarrow \infty$ . The frequency and space coordinates in the equation are dimensionless, the scales chosen being  $\omega_c$  and  $\lambda$ , respectively.

To summarize, the model is represented by four parameters viz.,  $\omega_c$ ,  $\omega_m$ ,  $\lambda$ ,  $\alpha$ . The first two represent (inverse) time scales.  $\omega_c^{-1}$  will be shown to scale as DeGennes's tube renewal time  $\tau_e$  in the entangled limit.  $\omega_m^{-1}$  will be shown to be related, but not identical to the terminal time beyond which the system starts behaving as a fluid, rather than an entangled polymeric system [5].  $\lambda$  is a characteristic interaction length scale, and given that we have here a continuum theory, it cannot be less than the length of a monomer, since the theory cannot represent molecular-level dynamics, as it is designed to describe physics at a longer length scale. The dimensionless parameter  $\alpha$  can be written as  $D/[\lambda^2\omega_c]$ , where  $D$  is the diffusion constant. Both  $\lambda$  and  $\omega_c$  could possess a molecular

weight dependence of their own, so that  $\alpha$  can display a dependence on molecular weight different than the scaling behavior of  $D$ .

Since we wish to study polymer melts undergoing shear experiments, where they are in contact with an energy reservoir (at constant temperature), the energy which is conserved is the Helmholtz free energy  $A = U - ST$  [7],  $S$  being the entropy and  $T$  the temperature. The entropy is given approximately as [8]

$$S = \int d^3s \int_{-\omega_m}^{\omega_m} \frac{d\omega}{2\pi} s(\mathbf{s}, \omega), \quad s(\mathbf{s}, \omega) \approx c(\mathbf{s}, \omega) \ln[c(\mathbf{s}, \omega)],$$

$$(1 + c') \ln(1 + c') \approx c' + \frac{c'^2}{2} - \frac{c'^3}{6} + \frac{c'^4}{12}. \quad (2)$$

The last of these equations indicates an expansion around  $\lambda^{-3}$ , which is identical to one in the units we have chosen. The linear terms will be ignored following convention, as they can be absorbed into the chemical potential  $\mu$ , required for number conservation. In the mean field approximation,  $\mu \equiv 0$ . In what follows, we shall drop the primes on the number concentration variable.

The goal of this communication is to compute the linear viscoelastic response of a polymeric system. This can be done following closely the analysis in our previous paper [1], to obtain an expression for the frequency-dependent stress  $\sigma(\omega)$ :

$$\sigma(\omega) = -i\omega C S(k=0, \omega) \epsilon(\omega),$$

$$C = \left( \frac{kT}{\omega_c \lambda^3} \right), \quad (3)$$

where  $S(k, \omega)$  is the two-point correlation function for the system. Note that since we chose to take temporal Fourier transforms with respect to  $\exp(-i\omega t)$ , our sign convention in the first of Eqs. (3) is opposite that in standard literature [5]. In general  $S(k, \omega)$  is given by

$$S(k, \omega) = [S_0^{-1}(k, \omega) - \Sigma(k, \omega)]^{-1},$$

$$S_0(k, \omega) = [-i\omega + s_0^{-1}(k)]^{-1},$$

$$s_0(k) = [1 + \sqrt{2}\alpha k^2 + 2\alpha^2 k^2 / (1 + \sqrt{2}k^2/\alpha)]^{-1}$$

$$\approx (1 + \alpha k^2)^{-1},$$

$$a = 2\sqrt{2}\alpha, \quad (4)$$

where as usual  $\Sigma$  denotes the self-energy. From Eq. (4), we see that  $a$  plays the role of a diffusion constant. But bearing in mind the discussion below Eq. (1), we expect its dependence on molecular weight to be different than the conventional diffusion constant  $D$ , due to the manner in which we have scaled our variables.

From Eqs. (3) and (4), we see that we need to evaluate the correlation function in the long wavelength limit. We can perform this calculation using a perturbation expansion with respect to the nonlinear terms, using standard methods from field theory. These are elementary extensions of the methods detailed in Ref. [1]. The vertices we obtain from Eq. (2) are

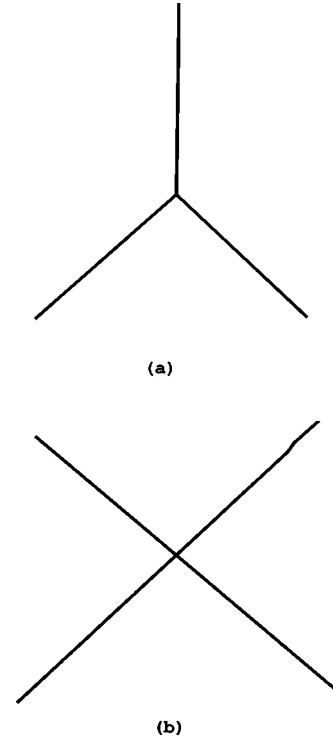


FIG. 1. (a) is a pictorial representation of the cubic term in  $A$ . Each leg corresponds to a factor of  $c$ , the field. The intersection of the three legs symbolizes a factor of  $\gamma = 1/6$ , the coupling constant. (b) is a pictorial representation of the quartic term in  $A$ . A factor of  $-1/12$  is to be inserted at the intersection.

depicted in Fig. 1 [9,10]. It is easy to show that the only surviving lowest order diagram is the setting-sun diagram Fig. 2, whose contribution can be shown analytically to be

$$\Sigma_{2b}(\omega, k=0, \omega_c, \omega_m)$$

$$= \frac{1}{4} \int \frac{d\omega'}{2\pi} \int \frac{d^3k}{(2\pi)^3} S_0(k, \omega') S_0(k, \omega - \omega')$$

$$= \frac{\sqrt{i\omega/\omega_c - 1}}{32\pi^2 a^{3/2}} \left\{ \ln \left[ \frac{(\omega/2 + \omega_m)(3\omega/2 - \omega_m)}{(\omega/2 - \omega_m)(3\omega/2 + \omega_m)} \right] \right\}. \quad (5)$$

Here  $\omega$  is the frequency at which the system is being sheared. In order to obtain the final expression for the self-energy in the long wavelength limit, we first performed the frequency integral. Next, to perform the  $k$  integration, we used the method of contour integration, taking care to distort the contour to avoid the branch cut implied by the logarithm.

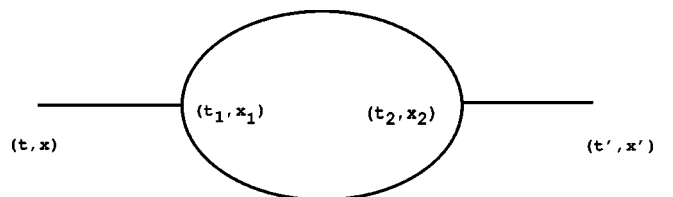


FIG. 2. This figure (the setting-sun diagram) represents the only lowest order nonvanishing contribution and arises from the cubic interaction term in the Free energy  $A$  [see Eq. (2)].

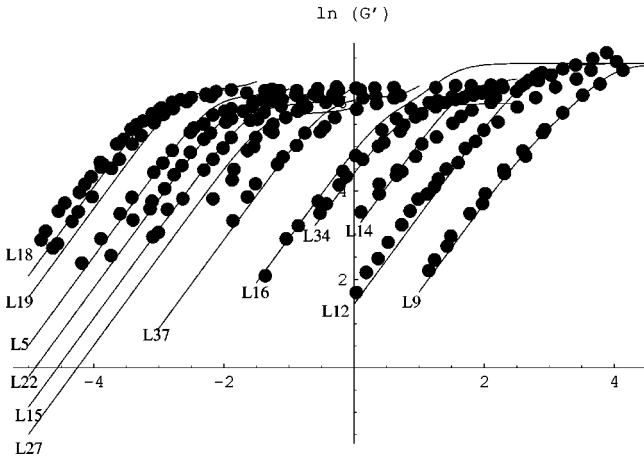


FIG. 3. This plot shows a comparison of our theory (solid line) with the experimental data by Onogi *et al.* on polystyrene melts. The comparison is fairly good for high  $M$ , and to deteriorates as the molecular weight decreases. The plateaus indicate the rubbery regime for each sample. Note that L18=581,000, L19=513,000, L5=351,000, L22=275,000, L15=215,000, L27=167,000, L37=113,000, L16=58700, L34=46900, L14=28900, L12=14800, and L9=8900. The data are labeled as done originally by Onogi *et al.* The plot is log-log, as a function of frequency  $\omega$ , to the base 10.

mic behavior of the integrand in  $k$  space. Then the method of residues yields the final expression in Eq. (5).

In the zero frequency limit the viscosity is given by

$$\eta_0 = \lim_{\omega \rightarrow 0} \omega^{-1} \text{Im}[-i\omega CS(k=0, \omega)] \equiv C. \quad (6)$$

We have four parameters in the theory, viz.,  $\lambda$ ,  $\alpha$ ,  $\omega_m$ , and  $\omega_c$ . To compare our theory with experimental results, we began by noting that Onogi *et al.* [11] have obtained values of the zero shear viscosity  $\eta_0$  as a function of the molecular weight  $M$  for polystyrene melts. For  $M > 30\,000$ , their data yields  $\eta_0 \sim M^{3.7}$ , consistent with other data in the literature. For  $M \leq 30\,000$ ,  $\eta_0 \sim M^{-1}$ . We parametrized their viscosity data, and used it as a constraint through Eq. (6), to fit data on the storage moduli of polystyrene melts with a low polydispersity (a few percent), and a fairly wide range of molecular weights, from 8900 to about 580 000 [11], utilizing Eqs. (3)–(5). Thus, while we can choose either  $\lambda$  or  $\omega_c$  independently, the other is determined automatically. This procedure automatically guarantees that the zero shear viscosity obtained from our theory satisfies conventional scaling laws. In doing these fits, we also ensured that the length scale was chosen to be no less than a few Å, which is what the length of the polystyrene monomer ( $\text{CH}_2-\text{COH}$ ) must be. Twelve sets of data are shown in Fig. 3, ranging from low to high molecular weight samples. The fits are good for  $M \geq 29\,000$ , for  $\omega \leq 1$ , and deteriorate for lower molecular weights. The plateaus indicate the rubbery phase of the system. Our previous paper applies in this region [1]. At the higher end of the frequency range (high strain rates), the stress is much higher, which could be interpreted in terms of inertia as the system starts to be strained. For frequencies below the plateaus (low strain rate), one might say that the

polymers eventually begin to disentangle, causing the stress to start decreasing precipitously.

While it is true that the parameters in our theory had to be chosen to get the best fit with data, subject to some constraints, we find it impressive that the function given in Eq. (5) is such that it provides the correct *form* for the storage modulus. In this sense, our theory has captured the essential aspects of the linear viscoelasticity of polymer melts. From the values obtained for the four parameters, we were able to perform a least-squares fit, yielding the following representations:

$$a \approx 2.43 \times 10^{-18} M^{2.3} \quad (\text{dimensionless}) \quad \forall M,$$

$$\omega_m \approx 1.11 \times 10^4 M^{-2.3} (\text{s}^{-1}) \quad \forall M \leq 3 \times 10^4,$$

$$\omega_m \approx 1.07 \times 10^{-8} \text{ s}^{-1} \quad \forall M > 3 \times 10^4,$$

$$\lambda = 20 \text{ \AA} \quad \forall M \leq 5.87 \times 10^4,$$

$$\lambda = 4 \text{ \AA} \quad \forall M > 5.87 \times 10^4. \quad (7)$$

Note that apart from  $a$  ( $\sim \alpha$ ), the other two parameters have different scaling forms, depending on whether the system is entangled, or unentangled (as a function of  $M$ ). In the fitting process, we found that adjusting  $\omega_m$  served to modify the shape of the storage modulus in the low frequency regime. In this sense, it is related to the terminal strain rate below which the system behaves as a fluid rather than an entangled system. It turns out that  $\omega_m$  ranges from  $10^{-10} \text{ s}^{-1}$  in the high- $M$  region to  $10^{-8} \text{ s}^{-1}$  in the low- $M$  regime. Adjusting  $\omega_m$  yields the experimentally determined terminal strain rate which follows the usual inverse cubic scaling law [11] as a function of  $M$ . The value of  $\lambda$  is of the order of a few Å in accordance with the earlier discussion. The fourth parameter  $\omega_c$  is determined from  $\lambda$  using Eq. (6). Notice that the ranges of  $M$  for which the representations of  $\lambda$  are different, is not the same as for  $\omega_m$ . We shall discuss the consequences of this below.

The advantage of our theory is that while reptation theory is restricted to the regime of highly entangled systems (high  $M$ ), and uses mean-field concepts such as a preformed tube, we can compute the effect of fluctuations using Feynman diagrams. Now, Onogi *et al.* [11] estimate that the onset of entanglement takes place at about  $M = 30\,000$ . There is a curious signature of this crossover to entanglement which arises out of our theory, besides the vanishing of the plateau in the storage modulus as a function of frequency. And that signature is a phenomenon analogous to critical slowing down in the theory of second order phase transitions. By this we mean that a plot of  $\omega_c$  as a function of the molecular weight  $M$  appears to display a minimum in the neighborhood of  $M \sim 30\,000$ . On either side of this minimum, of course,  $\omega_c$  will be higher. The partial evidence we have found for this phenomenon is displayed pictorially in Fig. 4, which is a plot of the characteristic frequency  $\omega_c$  versus  $M$ .

The functional dependence of  $\omega_c$  is determined from Eq. (6), once  $\lambda$  is chosen. The unentangled and entangled regimes are clearly visible on the log-log plot as straight line segments with slopes of  $M^{-1}$  and  $M^{-3.7}$ , respectively.  $\lambda$  is constant in each of these regimes. Thus  $\omega_c \sim M^{-3.7}$  in the entangled regime. On this basis, and using Eq. (6), we identify  $\omega_c^{-1}$  with de Gennes's tube renewal time  $\tau_t$  in the en-

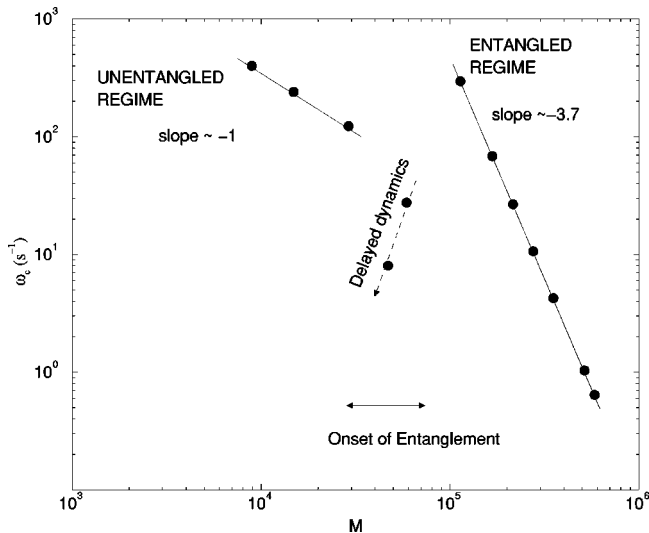


FIG. 4. This plot shows the behavior of  $\omega_c$  as a function of the molecular weight  $M$ . The unentangled and entangled states are denoted by straight lines on this log-log plot with slopes of  $-1$  and  $-3.7$ , respectively. An intermediate region, where entanglement sets in, is marked by a curiously low value of  $\omega_c$ , which is a signature that the dynamics of the system are slowing down tremendously.

tangled regime. The two dynamical regimes are separated by an interval which we associate with the onset of entanglement, where  $\omega_c$  dips rather dramatically as  $M$  decreases, from a value of about  $300 \text{ s}^{-1}$ , to a few Hz, for two samples with  $M = 46\,900$  and  $58\,700$ . If there were data available in the range of  $M = 30\,000$  to  $M = 46\,900$ , one might be able to resolve the minimum in  $\omega_c$ . We attempted adjusting the parameters to avoid this *anomalous* behavior, but could only do so for the longer sample. But that causes  $\omega_c$  to rise to about  $3425 \text{ Hz}$ , which begs the question why the time scale for this sample should be much smaller than that for  $M = 28\,900$ , which lies in the unentangled regime. The anomalous behavior in Fig. 4 can be traced to the fact that the experimental data for these two values of  $M$  cut across the curves for higher  $M$  samples. The dramatic increase in the (reptation) tube renewal time  $\omega_c^{-1}$  in the intermediate molecular weight regime is an indication of critical slowing down, which we anticipated in our earlier static theory [1]. Our results should stimulate further experiments in this regime in order to ensure the validity of this concept.

As advertised earlier, the dependence of  $a$  on  $M$  is different than that of the true diffusion constant  $D$ . The reason is that  $a$  is proportional to  $\alpha \equiv D\lambda^{-2}\omega_c^{-1}$ , and from our fits,  $D \sim M^{-1.3}$  in the high- $M$  regime. This scaling deviates from DeGennes's inverse quadratic law, and is due to the experimental scaling  $\eta_0 \sim M^{-p}$ , with  $p$  closer to 3.7 than the oft-quoted value 3 to 3.4. The low value of the diffusion constant which we obtain agrees fairly well with Graessley's formula [5], which yields  $D \sim \mathcal{O}(10^{-18}) \text{ cm}^2 \text{ s}^{-1}$  for  $M = 6 \times 10^5$ . In the low  $M$  regime,  $D \sim M^{+4/3}$ , which is not what one would expect. This occurs because our theory does not apply in the low  $M$  regime, as we were unable to get reasonable fits in that regime.

As one might perhaps expect, the entropy terms in our energy functional have a dominant effect on determining the linear viscoelastic behavior of polystyrene melts. The nonlocal attractive term, which models the resistance to the motion of entangled polymers has a less pronounced effect on linear viscoelasticity. This is consistent with our earlier calculations in the static regime [1], where we found that the nonlocal attractive term has a profound effect on determining the renormalized diffusion constant than the elastic moduli. We will tackle the frequency dependence of the renormalized diffusion constant in future work.

With these parametric representations, we were also able to compute the loss moduli for the samples. The curves gave a reasonable but only an average fit for the various samples. In other words, the loss moduli obtained through our procedure was not very sensitive to the parameters we obtained. Nevertheless, we note that this is an improvement over the standard reptation model approaches, which give a null loss modulus [5].

In this paper we have presented a field-theoretic analysis, including the effect of fluctuations, of the data of Onogi *et al.* [11] on the storage moduli of polystyrene melts for a wide range of molecular weights, and we find that analogous to dynamic critical phenomena [12], the onset of entanglement is characterized by critical slowing down. Our result should stimulate further experiments in this regime in order to ensure the validity of this concept.

This research was supported by U.S. Department of Energy Contract No. W-7405-ENG-36 under the aegis of the Los Alamos National Laboratory LDRD polymer aging DR program.

- 
- [1] S.M. Chitanvis, *Phys. Rev. E* **58**, 3469 (1998).  
 [2] Y. Termonia and P. Smith, *Macromolecules* **20**, 835 (1987); **29**, 4891 (1996).  
 [3] J. Bicerano, N.K. Grant, J.T. Seitz, and K. Pant, *J. Polym. Sci., Part B: Polym. Phys.* **35**, 2715 (1997).  
 [4] T. Holtzl, H.L. Trautenberg, and D. Goritz, *Phys. Rev. Lett.* **79**, 2299 (1997).  
 [5] M. Doi and S.F. Edwards, *The Theory of Polymer Dynamics*, (Oxford University Press, Oxford, 1986).  
 [6] J.W. Cahn and J.E. Hilliard, *J. Chem. Phys.* **28**, 258 (1958).  
 [7] H.B. Callen, *Thermodynamics* (Wiley, New York, 1960), p.106.  
 [8] H.J. Raveché, *J. Chem. Phys.* **55**, 2242 (1971).  
 [9] P. Ramond, *Field Theory: A Modern Primer* (Benjamin/Cummings, New York, 1981), p. 126.  
 [10] J.J. Binney, N.J. Dowrick, A.J. Fisher, and M.E.J. Newman, *The Theory of Critical Phenomena: An Introduction to the Renormalization Group* (Oxford Science, Oxford, 1995).  
 [11] S. Onogi, T. Masuda, and K. Kitagawa, *Macromolecules* **3**, 109 (1970).  
 [12] P.C. Hohenberg and B.I. Halperin, *Rev. Mod. Phys.* **49**, 435 (1977).